

A new innovative 3-unknowns HSDT for buckling and free vibration of exponentially graded sandwich plates resting on elastic foundations under various boundary conditions

Mohamed Rabhi¹, Kouider Halim Benrahou^{*1}, Abdelhakim Kaci^{1,2}, Mohammed Sid Ahmed Houari³, Fouad Bourada^{1,4}, Abdelmoumen Anis Bousahla⁵, Abdeldjebbar Tounsi¹, E.A. Adda Bedia⁶, S.R. Mahmoud⁷ and Abdelouahed Tounsi^{*,1,6}

¹Department of Civil Engineering, Material and Hydrology Laboratory, University of Sidi Bel Abbes, Faculty of Technology, Algeria

²Department of Civil and Hydraulic Engineering, Dr Tahar Moulay University, Faculty of Technology, BP 138 Cité En-Nasr 20000, Saida, Algeria

³Faculty of Science and Technology, Mascara University, Mascara 29000, Algeria

⁴Department of Science and Technology, Tissemsilt University Center, BP 38004 Ben Hamouda, Algeria

⁵Multi-scale Modeling and Simulation Laboratory, University of Sidi Bel Abbès, Algeria

⁶Department of Civil and Environmental Engineering, King Fahd University of Petroleum & Minerals, 31261 Dhahran, Eastern Province, Saudi Arabia

⁷GRC Department, Jeddah Community College, King Abdulaziz University, Jeddah, Saudi Arabia

(Received April 2, 2020, Revised May 25, 2020, Accepted June 8, 2020)

Abstract. In this study a new innovative three unknowns trigonometric shear deformation theory is proposed for the buckling and vibration responses of exponentially graded sandwich plates resting on elastic mediums under various boundary conditions. The key feature of this theoretical formulation is that, in addition to considering shear deformation effect, it has only three unknowns in the displacement field as in the case of the classical plate theory (CPT), contrary to five as in the first shear deformation theory (FSDT) and higher-order shear deformation theory (HSDT). Material characteristics of the sandwich plate faces are considered to vary within the thickness direction via an exponential law distribution as a function of the volume fractions of the constituents. Equations of motion are obtained by employing Hamilton's principle. Numerical results for buckling and free vibration analysis of exponentially graded sandwich plates under various boundary conditions are obtained and discussed. Verification studies confirmed that the present three -unknown shear deformation theory is comparable with higher-order shear deformation theories which contain a greater number of unknowns.

Keywords: functionally graded materials; sandwich plates; a 3-unknown theory; various boundary conditions; elastic; foundations; free vibration; buckling loads

1. Introduction

In recent years, the use of functionally graded (FG) sandwich structures in engineering fields such as civil engineering, aerospace, shipbuilding and machinery sectors has attracted intensive research interests due to their high strength-to-weight ratio. As a result, the mechanical response of FG sandwich structures is of considerable importance in both academic research and industrial fields (Sofiyev *et al.* 2012, Yaghoobi and Yaghoobi 2013, Swaminathan and Naveenkumar 2014, Kar and Panda 2015, Ahmed *et al.* 2019, Mehar and Panda 2018, Rezaiee-Pajand *et al.* 2018, Dash *et al.* 2018, Karami *et al.* 2019, Mehar *et al.* 2019 and 2020, Avcar 2019, Kirlangiç and Akbaş 2020). Since the shear deformation influences are considerably important in thick plates or plates manufactured of FGMs,

shear deformation theories such as first-order shear deformation theory (FSDT) and higher-order shear deformation theories (HSDTs) should be utilized to investigate the mechanical responses of FG plates.

The FSDT generates reasonable results, but requires the use of a shear correction parameter (Civalek and Acar 2007, Mousavi and Tahani 2012, Malekzadeh and Monajjemzadeh 2013, Avcar 2016, Shokravi 2017, Hamidi *et al.* 2018, Bensattalah *et al.* 2019, Mirjavadi *et al.* 2019a). Whereas, the HSDTs (Touratier 1991, Soldatos 1992, Reddy 2000, Karama *et al.* 2003, Pradyumna and Bandyopadhyay 2008, Talha and Singh 2010, Sobhy 2013, Panda and Katariya 2015, Katariya and Panda 2016, Mehar *et al.* 2016 and 2017, Kar and Panda 2017, Katariya *et al.* 2017, Katariya and Panda 2019ab and 2020, Mehar and Panda 2019, Katariya *et al.* 2018 and 2019, Abdulrazzaq *et al.* 2020) do not need a shear correction parameter, but their governing equations are more complex than those of the FSDT.

Recently, new shear deformation theories involving only four unknowns have been developed (Ghugal and Sayyad 2011, Nguyen 2014, Zhang *et al.* 2015, Sobhy 2016, Adim *et al.* 2016, Abdelmalek *et al.* 2017, Zouatnia *et al.* 2018),

*Corresponding author, Professor
E-mail: kbenrahouhalim@gmail.com

**Corresponding author, Professor
E-mail: tou_abdel@yahoo.com

but these theories lead to the resolution of a number of equations of motion more than of those used in classical plate theory (CPT) (Akgoz and Civalek 2011, Avcar and Mohammed 2018). Thus, needs exist for the development of HSDTs which are simple to use.

In the present work, an efficient and simple formulation with shear deformation effect is developed for the buckling and vibrational analyses of exponentially graded sandwich plates resting on elastic foundations under various boundary conditions. The highlight of this new formulation is that, in addition to incorporating the shear deformation effect, the displacement components are expressed with only three unknowns as the classical plate theory (CPT), which is even less than the FSDT and do not requires shear correction parameter. The sandwich plate is considered to be supported by isotropic or orthotropic two-parameter elastic foundations. The equations of motion of exponentially graded sandwich plates resting on elastic foundation are obtained by utilizing the Hamilton's principle. These equations of motion for the sandwich plate under various boundary conditions are then solved. As a result, critical buckling loads and natural frequencies are determined by solving eigenvalue problem. The performance of the present formulation is verified by comparing it with HSDT's solutions available in literature. It can be concluded that the present method is as accurate as other HSDTs with higher number of unknowns and so deserves attention.

2. Theoretical formulation

Consider a sandwich plate with three layers as depicted in Fig. 1. Two FG face sheets are synthesized of a mixture of a metal and a ceramic, while the core is manufactured from an isotropic homogeneous material. The material properties \bar{P} of FG face sheets such as Young's modulus E and the material density ρ , are supposed to vary continuously within the plate thickness by an exponential law distribution as (Sobhy 2013):

$$\bar{P}^{(n)}(z) = \bar{P}_m \exp(\beta V^{(n)}), \quad \beta = \ln\left(\frac{\bar{P}_c}{\bar{P}_m}\right), \quad (n=1, 2, 3) \quad (1)$$

where subscripts m and c refer to metal and ceramic, and the volume fraction $V^{(n)}$ of each layer is given by:

$$V^{(1)} = \left(\frac{2\bar{z}+1}{2\bar{h}_1+1}\right)^k, \quad -1/2 \leq \bar{z} \leq \bar{h}_1 \quad (2a)$$

$$V^{(2)} = 1, \quad \bar{h}_1 \leq \bar{z} \leq \bar{h}_2 \quad (2b)$$

$$V^{(3)} = \left(\frac{2\bar{z}-1}{2\bar{h}_2-1}\right)^k, \quad \bar{h}_2 \leq \bar{z} \leq 1/2 \quad (2c)$$

where $\bar{z} = z/h$, $\bar{h}_i = h_i/h$ ($i=$) and k is the inhomogeneity parameter which takes values greater than or equal to zero. It is noted that the core is independent of the value of k which is fully ceramic.

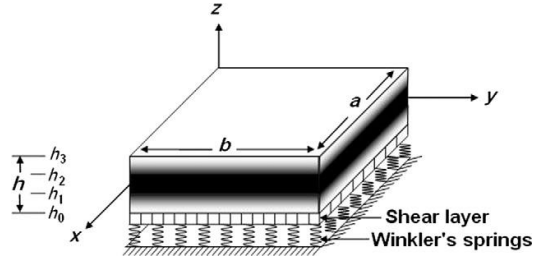


Fig. 1 Geometry of the exponentially graded sandwich plate resting on elastic foundations

2.1 Kinematics and constitutive equations

The displacement field of the novel theory is given as follows:

$$\begin{aligned} u(x, y, z, t) &= u_0(x, y, t) - z \frac{\partial w_0}{\partial x} - \beta f(z) \frac{\partial^3 w_0}{\partial x^3} \\ v(x, y, z, t) &= v_0(x, y, t) - z \frac{\partial w_0}{\partial y} - \beta f(z) \frac{\partial^3 w_0}{\partial y^3} \\ w(x, y, z, t) &= w_0(x, y, t) \end{aligned} \quad (3)$$

where u_0 , v_0 , and w_0 are three unknown displacement functions of middle surface of the plate and β is a parameter of the present displacement model.

In this work the displacement field contains a shape functions expressed as:

$$f(z) = \frac{h}{\pi} \sin \frac{\pi z}{h} \quad (4)$$

The nonzero linear strains associated with the displacement field in Eq. (3) are

$$\begin{aligned} \begin{Bmatrix} \varepsilon_x \\ \varepsilon_y \\ \gamma_{xy} \end{Bmatrix} &= \begin{Bmatrix} \varepsilon_x^0 \\ \varepsilon_y^0 \\ \gamma_{xy}^0 \end{Bmatrix} + z \begin{Bmatrix} k_x \\ k_y \\ k_{xy} \end{Bmatrix} + \beta f(z) \begin{Bmatrix} \eta_x \\ \eta_y \\ \eta_{xy} \end{Bmatrix}, \\ \begin{Bmatrix} \gamma_{yz} \\ \gamma_{xz} \end{Bmatrix} &= \beta g(z) \begin{Bmatrix} \gamma_{yz}^0 \\ \gamma_{xz}^0 \end{Bmatrix}, \end{aligned} \quad (5)$$

where

$$\begin{aligned} \begin{Bmatrix} \varepsilon_x^0 \\ \varepsilon_y^0 \\ \gamma_{xy}^0 \end{Bmatrix} &= \begin{Bmatrix} \frac{\partial u_0}{\partial x} \\ \frac{\partial v_0}{\partial x} \\ \frac{\partial u_0}{\partial y} + \frac{\partial v_0}{\partial x} \end{Bmatrix}, \quad \begin{Bmatrix} k_x \\ k_y \\ k_{xy} \end{Bmatrix} = \begin{Bmatrix} -\frac{\partial^2 w_0}{\partial x^2} \\ -\frac{\partial^2 w_0}{\partial y^2} \\ -2\frac{\partial^2 w_0}{\partial x \partial y} \end{Bmatrix}, \\ \begin{Bmatrix} \eta_x \\ \eta_y \\ \eta_{xy} \end{Bmatrix} &= \begin{Bmatrix} -\frac{\partial^4 w_0}{\partial x^4} \\ -\frac{\partial^4 w_0}{\partial y^4} \\ -\frac{\partial^2 (\nabla^2 w_0)}{\partial x \partial y} \end{Bmatrix}, \quad \begin{Bmatrix} \gamma_{yz}^0 \\ \gamma_{xz}^0 \end{Bmatrix} = \begin{Bmatrix} -\frac{\partial^3 w_0}{\partial y^3} \\ -\frac{\partial^3 w_0}{\partial x^3} \end{Bmatrix}, \end{aligned} \quad (6)$$

and

$$g(z) = f'(z), \quad \nabla^2 w_0 = \frac{\partial^2 w_0}{\partial x^2} + \frac{\partial^2 w_0}{\partial y^2} \quad (7)$$

For the exponentially graded sandwich plates, the stress-strain relationships can be written as:

$$\begin{Bmatrix} \sigma_x \\ \sigma_y \\ \tau_{yz} \\ \tau_{xz} \\ \tau_{xy} \end{Bmatrix}^{(n)} = \begin{bmatrix} C_{11} & C_{12} & 0 & 0 & 0 \\ C_{12} & C_{22} & 0 & 0 & 0 \\ 0 & 0 & C_{44} & 0 & 0 \\ 0 & 0 & 0 & C_{55} & 0 \\ 0 & 0 & 0 & 0 & C_{66} \end{bmatrix}^{(n)} \begin{Bmatrix} \varepsilon_x \\ \varepsilon_y \\ \gamma_{yz} \\ \gamma_{xz} \\ \gamma_{xy} \end{Bmatrix} \quad (8)$$

where $(\sigma_x, \sigma_y, \sigma_z, \tau_{yz}, \tau_{xz}, \tau_{xy})$ and $(\varepsilon_x, \varepsilon_y, \varepsilon_z, \gamma_{yz}, \gamma_{xz}, \gamma_{xy})$ are the stress and strain components, respectively. The elastic constants C_{ij} are defined as

$$\begin{aligned} C_{11}^{(n)} &= C_{22}^{(n)} = \frac{E^{(n)}(z)}{1-\nu^2}, \quad C_{12}^{(n)} = \nu C_{11}^{(n)}, \\ C_{44}^{(n)} &= C_{55}^{(n)} = C_{66}^{(n)} = \frac{E^{(n)}(z)}{2(1+\nu)}, \end{aligned} \quad (9)$$

2.2 Equations of motion

Hamilton's principle is utilized herein to determine equations of motion. The principle can be stated in an analytical form as follows (Ebrahimi and Barati 2017a, Eltaher *et al.* 2018, Hadji *et al.* 2019, Sahouane *et al.* 2019, Fenjan *et al.* 2019ab, Safa *et al.* 2019, Mirjavadi *et al.* 2019b, Hamed *et al.* 2020, Eltaher and Mohamed 2020):

$$\delta \int_0^T (\delta U + \delta V - \delta K) dt \quad (10)$$

where δU is the variation of strain energy; δV is the variation of work induced by the external forces; and δK is the variation of kinetic energy.

The variation of strain energy of the plate is calculated by

$$\begin{aligned} \delta U &= \int_V [\sigma_x \delta \varepsilon_x + \sigma_y \delta \varepsilon_y + \tau_{xy} \delta \gamma_{xy} + \tau_{yz} \delta \gamma_{yz} + \tau_{xz} \delta \gamma_{xz}] dV \\ &= \int_A [N_x \delta \varepsilon_x^0 + N_y \delta \varepsilon_y^0 + N_{xy} \delta \gamma_{xy}^0 + M_x \delta k_x + M_y \delta k_y + M_{xy} \delta k_{xy} \\ &\quad + \beta (S_x \delta \eta_x + S_y \delta \eta_y + S_{xy} \delta \eta_{xy} + Q_{yz} \delta \gamma_{yz}^0 + Q_{xz} \delta \gamma_{xz}^0)] dA = 0 \end{aligned} \quad (11)$$

where A is the top surface and the stress resultants N , M , S and Q are defined by:

$$\begin{aligned} (N_i, M_i, S_i) &= \sum_{n=1}^3 \int_{h_{n-1}}^{h_n} (1, z, \beta f) (\sigma_i) dz, \quad (i = x, y, xy) \quad \text{and} \\ Q_i &= \sum_{n=1}^3 (\tau_i) \beta g(z) dz, \quad (i = xz, yz) \end{aligned} \quad (12)$$

The variation of work done by the applied loads can be expressed as

$$\delta V = - \int_A (P - f_e) \delta (w_b + w_s) dA \quad (13)$$

where f_e is the density of reaction force of foundation. For the Pasternak foundation model:

$$f_e = K_W w - K_{S1} \frac{\partial^2 w}{\partial x^2} - K_{S2} \frac{\partial^2 w}{\partial y^2} \quad (14)$$

where K_W is the modulus of subgrade reaction (elastic coefficient of the foundation) and K_{S1} and K_{S2} are the shear moduli of the subgrade (shear layer foundation stiffness). If foundation is homogeneous and isotropic, we will get $K_{S1} = K_{S2} = K_S$. If the shear layer foundation stiffness is neglected, Pasternak foundation becomes a Winkler foundation with

$$P = \left[P_x^0 \frac{\partial^2 w}{\partial x^2} + P_y^0 \frac{\partial^2 w}{\partial y^2} + 2P_{xy}^0 \frac{\partial^2 w}{\partial x \partial y} \right] \quad (15)$$

The variation of kinetic energy is written as

$$\begin{aligned} \delta K &= \int_V [\dot{u} \delta \dot{u} + \dot{v} \delta \dot{v} + \dot{w} \delta \dot{w}] \rho(z) dV \\ &= \int_A \left\{ I_0 [\dot{u}_0 \delta \dot{u}_0 + \dot{v}_0 \delta \dot{v}_0 + \dot{w}_0 \delta \dot{w}_0] \right. \\ &\quad - I_1 \left(\dot{u}_0 \frac{\partial \delta \dot{w}_0}{\partial x} + \frac{\partial \dot{w}_0}{\partial x} \delta \dot{u}_0 + \dot{v}_0 \frac{\partial \delta \dot{w}_0}{\partial y} + \frac{\partial \dot{w}_0}{\partial y} \delta \dot{v}_0 \right) \\ &\quad - J_1 \beta \left(\dot{u}_0 \frac{\partial^3 \delta \dot{w}_0}{\partial x^3} + \frac{\partial^3 \dot{w}_0}{\partial x^3} \delta \dot{u}_0 + \dot{v}_0 \frac{\partial^3 \delta \dot{w}_0}{\partial y^3} + \frac{\partial^3 \dot{w}_0}{\partial y^3} \delta \dot{v}_0 \right) \\ &\quad + I_2 \left(\frac{\partial \dot{w}_0}{\partial x} \frac{\partial \delta \dot{w}_0}{\partial x} + \frac{\partial \dot{w}_0}{\partial y} \frac{\partial \delta \dot{w}_0}{\partial y} \right) \\ &\quad + K_2 \beta^2 \left(\frac{\partial^3 \dot{w}_0}{\partial x^3} \frac{\partial^3 \delta \dot{w}_0}{\partial x^3} + \frac{\partial^3 \dot{w}_0}{\partial y^3} \frac{\partial^3 \delta \dot{w}_0}{\partial y^3} \right) \\ &\quad \left. + J_2 \beta \left(\frac{\partial \dot{w}_0}{\partial x} \frac{\partial^3 \delta \dot{w}_0}{\partial x^3} + \frac{\partial^3 \dot{w}_0}{\partial x^3} \frac{\partial \delta \dot{w}_0}{\partial x} + \frac{\partial \dot{w}_0}{\partial y} \frac{\partial^3 \delta \dot{w}_0}{\partial y^3} + \frac{\partial^3 \dot{w}_0}{\partial y^3} \frac{\partial \delta \dot{w}_0}{\partial y} \right) \right\} dA \end{aligned} \quad (16)$$

where dot-superscript convention indicates the differentiation with respect to the time variable t ; $\rho(z)$ is the mass density; and $(I_0, I_1, J_1, I_2, J_2, K_2)$ are mass inertias defined as

$$(I_0, I_1, J_1, I_2, J_2, K_2) = \sum_{n=1}^3 \int_{h_{n-1}}^{h_n} (1, z, f, z^2, z f, f^2) \rho(z) dz \quad (17)$$

Using the expressions for δU , δV , and δK from Eqs. (11), (14), and (16) into Eq. (10) and integrating by parts, and collecting the coefficients of δu_0 , δv_0 and δw_0 , the following equations of motion of the plate are obtained

$$\begin{aligned} \delta u_0: \quad & \frac{\partial N_x}{\partial x} + \frac{\partial N_{xy}}{\partial y} = I_0 \ddot{u}_0 - I_1 \frac{\partial \ddot{w}_0}{\partial x} - \beta J_1 \frac{\partial^3 \ddot{w}_0}{\partial x^3} \\ \delta v_0: \quad & \frac{\partial N_{xy}}{\partial x} + \frac{\partial N_y}{\partial y} = I_0 \ddot{v}_0 - I_1 \frac{\partial \ddot{w}_0}{\partial y} - \beta J_1 \frac{\partial^3 \ddot{w}_0}{\partial y^3} \\ \delta w_0: \quad & \frac{\partial^2 M_x}{\partial x^2} + 2 \frac{\partial^2 M_{xy}}{\partial x \partial y} + \frac{\partial^2 M_y}{\partial y^2} \\ & + \beta \left(\frac{\partial^4 S_x}{\partial x^4} + \frac{\partial^4 S_{xy}}{\partial x^3 \partial y} + \frac{\partial^4 S_{xy}}{\partial y^3 \partial x} + \frac{\partial^4 S_y}{\partial y^4} - \frac{\partial^3 Q_{xz}}{\partial x^3} - \frac{\partial^3 Q_{yz}}{\partial y^3} \right) \\ & - P - f_e = I_0 \ddot{w}_0 + I_1 \left(\frac{\partial \ddot{u}_0}{\partial x} + \frac{\partial \ddot{v}_0}{\partial y} \right) - I_2 \left(\frac{\partial^2 \ddot{w}_0}{\partial x^2} + \frac{\partial^2 \ddot{w}_0}{\partial y^2} \right) \\ & + \beta J_1 \left(\frac{\partial^3 \ddot{u}_0}{\partial x^3} + \frac{\partial^3 \ddot{v}_0}{\partial y^3} \right) - 2\beta J_2 \left(\frac{\partial^4 \ddot{w}_0}{\partial x^4} + \frac{\partial^4 \ddot{w}_0}{\partial y^4} \right) - \beta^2 K_2 \left(\frac{\partial^6 \ddot{w}_0}{\partial x^6} + \frac{\partial^6 \ddot{w}_0}{\partial y^6} \right) \end{aligned} \quad (18)$$

Substituting Eq. (5) into Eq. (8) and the subsequent results into Eqs. (12), the following constitutive equations are found:

$$\begin{Bmatrix} N_x \\ N_y \\ N_{xy} \\ M_x \\ M_y \\ M_{xy} \\ S_x \\ S_y \\ S_{xy} \end{Bmatrix} = \begin{bmatrix} A_{11} & A_{12} & 0 & B_{11} & B_{12} & 0 & \beta B_{11}^s & \beta B_{12}^s & 0 \\ A_{12} & A_{22} & 0 & B_{12} & B_{22} & 0 & \beta B_{12}^s & \beta B_{22}^s & 0 \\ 0 & 0 & A_{66} & 0 & 0 & B_{66} & 0 & 0 & \beta B_{66}^s \\ B_{11} & B_{12} & 0 & D_{11} & D_{12} & 0 & \beta D_{11}^s & \beta D_{12}^s & 0 \\ B_{12} & B_{22} & 0 & D_{12} & D_{22} & 0 & \beta D_{12}^s & \beta D_{22}^s & 0 \\ 0 & 0 & B_{66} & 0 & 0 & D_{66} & 0 & 0 & \beta D_{66}^s \\ \beta B_{11}^s & \beta B_{12}^s & 0 & \beta D_{11}^s & \beta D_{12}^s & 0 & \beta^2 H_{11}^s & \beta^2 H_{12}^s & 0 \\ \beta B_{12}^s & \beta B_{22}^s & 0 & \beta D_{12}^s & \beta D_{22}^s & 0 & \beta^2 H_{12}^s & \beta^2 H_{22}^s & 0 \\ 0 & 0 & \beta B_{66}^s & 0 & 0 & \beta D_{66}^s & 0 & 0 & \beta^2 H_{66}^s \end{bmatrix} \begin{Bmatrix} \varepsilon_x^0 \\ \varepsilon_y^0 \\ \gamma_{xy}^0 \\ k_x \\ k_y \\ k_{xy} \\ \eta_x \\ \eta_y \\ \eta_{xy} \end{Bmatrix} \quad (19a)$$

$$\begin{Bmatrix} Q_{xz} \\ Q_{yz} \end{Bmatrix} = \beta^2 \begin{bmatrix} A_{55}^s & 0 \\ 0 & A_{44}^s \end{bmatrix} \begin{Bmatrix} \gamma_{xz}^0 \\ \gamma_{yz}^0 \end{Bmatrix} \quad (19b)$$

where

$$\begin{Bmatrix} A_{11} & B_{11} & D_{11} & B_{11}^s & D_{11}^s & H_{11}^s \\ A_{12} & B_{12} & D_{12} & B_{12}^s & D_{12}^s & H_{12}^s \\ A_{66} & B_{66} & D_{66} & B_{66}^s & D_{66}^s & H_{66}^s \end{Bmatrix} = \sum_{n=1}^3 \int_{h_{n-1}}^{h_n} C_{11} \left(1, z, z^2, f(z), z f(z), f^2(z) \right) \begin{Bmatrix} 1 \\ \nu \\ \frac{1-\nu}{2} \end{Bmatrix} dz \quad (20a)$$

$$(A_{22}, B_{22}, D_{22}, B_{22}^s, D_{22}^s, H_{22}^s) = (A_{11}, B_{11}, D_{11}, B_{11}^s, D_{11}^s, H_{11}^s) \quad (20b)$$

$$A_{44}^s = A_{55}^s = \sum_{n=1}^3 \int_{h_{n-1}}^{h_n} C_{44} [g(z)]^2 dz, \quad (20c)$$

The equations of motion of the present three-unknown trigonometric shear deformation theory can be written in terms of displacements (u_0 , v_0 and w_0) by substituting Eq.(6) into Eqs. (19) and the subsequent results into Eq. (18)

$$A_{11} \frac{\partial^2 u_0}{\partial x^2} + A_{66} \frac{\partial^2 u_0}{\partial y^2} + (A_{12} + A_{66}) \frac{\partial^2 v_0}{\partial x \partial y} - B_{11} \frac{\partial^3 w}{\partial x^3} - (B_{12} + 2B_{66}) \frac{\partial^3 w}{\partial x \partial y^2} - \beta \left(B_{66}^s \frac{\partial^5 w}{\partial x^2 \partial y^2} + (B_{12}^s + B_{66}^s) \frac{\partial^5 w}{\partial x \partial y^4} + B_{11}^s \frac{\partial^5 w}{\partial x^5} \right) = \quad (21a)$$

$$I_0 \ddot{u}_0 - I_1 \frac{\partial \ddot{w}_0}{\partial x} - \beta J_1 \frac{\partial^3 \ddot{w}_0}{\partial x^3} \\ A_{22} \frac{\partial^2 v_0}{\partial y^2} + A_{66} \frac{\partial^2 v_0}{\partial x^2} + (A_{12} + A_{66}) \frac{\partial^2 u_0}{\partial x \partial y} - B_{22} \frac{\partial^3 w}{\partial y^3} - (B_{12} + 2B_{66}) \frac{\partial^3 w}{\partial x^2 \partial y} - \beta \left(B_{66}^s \frac{\partial^5 w}{\partial x^2 \partial y^3} + (B_{12}^s + B_{66}^s) \frac{\partial^5 w}{\partial x^4 \partial y} + B_{22}^s \frac{\partial^5 w}{\partial y^5} \right) = \quad (21b)$$

$$I_0 \ddot{v}_0 - I_1 \frac{\partial \ddot{w}_0}{\partial y} - \beta J_1 \frac{\partial^3 \ddot{w}_0}{\partial y^3} \\ B_{11} \frac{\partial^3 u_0}{\partial x^3} + (B_{12} + 2B_{66}) \frac{\partial^3 u_0}{\partial x \partial y^2} + (B_{12} + 2B_{66}) \frac{\partial^3 v_0}{\partial x^2 \partial y} + B_{22} \frac{\partial^3 v_0}{\partial y^3} - D_{11} \frac{\partial^4 w_0}{\partial x^4} - 2(D_{12} + 2D_{66}) \frac{\partial^4 w_0}{\partial x^2 \partial y^2} - D_{22} \frac{\partial^4 w_0}{\partial y^4} + \beta \left[B_{11}^s \frac{\partial^5 u_0}{\partial x^5} + (B_{12}^s + B_{66}^s) \frac{\partial^5 u_0}{\partial x \partial y^4} + (B_{12}^s + B_{66}^s) \frac{\partial^5 v_0}{\partial x^4 \partial y} + B_{22}^s \frac{\partial^5 v_0}{\partial y^5} + B_{66}^s \frac{\partial^5 u_0}{\partial x^3 \partial y^2} + B_{66}^s \frac{\partial^5 v_0}{\partial x^2 \partial y^3} \right] \quad (21c)$$

$$-2D_{11}^s \frac{\partial^6 w_0}{\partial x^6} - 2(D_{12}^s + 2D_{66}^s) \frac{\partial^6 w_0}{\partial x^2 \partial y^4} - 2(D_{12}^s + 2D_{66}^s) \frac{\partial^6 w_0}{\partial x^4 \partial y^2} - 2D_{22}^s \frac{\partial^6 w_0}{\partial y^6} \Big] - \beta^2 \left[H_{11}^s \frac{\partial^8 w_0}{\partial x^8} + 2(H_{12}^s + H_{66}^s) \frac{\partial^8 w_0}{\partial x^4 \partial y^4} + H_{66}^s \frac{\partial^8 w_0}{\partial x^6 \partial y^2} + H_{66}^s \frac{\partial^8 w_0}{\partial x^2 \partial y^6} + H_{22}^s \frac{\partial^8 w_0}{\partial y^8} - A_{44}^s \frac{\partial^6 w_0}{\partial x^6} - A_{55}^s \frac{\partial^6 w_0}{\partial y^6} \right] - P - f_e = I_0 \ddot{w}_0 + I_1 \left(\frac{\partial \ddot{u}_0}{\partial x} + \frac{\partial \ddot{v}_0}{\partial y} \right) - I_2 \left(\frac{\partial^2 \ddot{w}_0}{\partial x^2} + \frac{\partial^2 \ddot{w}_0}{\partial y^2} \right) + \beta J_1 \left(\frac{\partial^3 \ddot{u}_0}{\partial x^3} + \frac{\partial^3 \ddot{v}_0}{\partial y^3} \right) - 2\beta J_2 \left(\frac{\partial^4 \ddot{w}_0}{\partial x^4} + \frac{\partial^4 \ddot{w}_0}{\partial y^4} \right) - \beta^2 K_2 \left(\frac{\partial^6 \ddot{w}_0}{\partial x^6} + \frac{\partial^6 \ddot{w}_0}{\partial y^6} \right) \quad (21c)$$

3. Analytical solutions

The analytical solution of Eq. (21) can be determined for sandwich plates under various boundary conditions by employing the following expansions of generalized displacements:

$$\begin{Bmatrix} u_0 \\ v_0 \\ w_0 \end{Bmatrix} = \begin{Bmatrix} U_{mn} \frac{\partial X_m(x)}{\partial x} Y_n(y) e^{i\omega t} \\ V_{mn} X_m(x) \frac{\partial Y_n(y)}{\partial y} e^{i\omega t} \\ W_{mn} X_m(x) Y_n(y) e^{i\omega t} \end{Bmatrix} \quad (22)$$

where $i = \sqrt{-1}$, (U_{mn} , V_{mn} , W_{mn}) are coefficients, and $\omega = \omega_{mn}$ denotes the eigenfrequency associated with $(m, n)^{th}$ eigenmode. The functions $X_m(x)$ and $Y_n(y)$ are suggested by Sobhy (2013) to satisfy various boundary conditions, and they are listed in Table 1 noting that $\lambda = m\pi/a$ and $\mu = n\pi/b$.

Substituting expressions (22) into Eqs. (21) and multiplying each equation by the corresponding eigenfunction then integrating over the domain of solution, we can determine, after some mathematical manipulations, the following expressions:

$$\begin{pmatrix} S_{11} & S_{12} & S_{13} \\ S_{12} & S_{22} & S_{23} \\ S_{13} & S_{23} & S_{33} \end{pmatrix} - \omega^2 \begin{pmatrix} m_{11} & 0 & m_{13} \\ 0 & m_{22} & m_{23} \\ m_{13} & m_{23} & m_{33} \end{pmatrix} \begin{Bmatrix} U_{mn} \\ V_{mn} \\ W_{mn} \end{Bmatrix} = \begin{Bmatrix} 0 \\ 0 \\ 0 \end{Bmatrix} \quad (23)$$

in which:

$$\begin{aligned} S_{11} &= A_{11}\alpha_{12} + A_{66}\alpha_8 \\ S_{12} &= (A_{12} + A_{66})\alpha_8 \\ S_{13} &= -B_{11}\alpha_{12} - (B_{12} + 2B_{66})\alpha_8 \\ &\quad - \beta \left(B_{11}^s\alpha_{15} + (B_{12}^s + B_{66}^s)\alpha_{14} + B_{66}^s\alpha_{28} \right) \\ S_{21} &= (A_{12} + A_{66})\alpha_{10} \\ S_{22} &= A_{22}\alpha_4 + A_{66}\alpha_{10} \\ S_{23} &= -B_{11}\alpha_4 - (B_{12} + 2B_{66})\alpha_{10} \\ &\quad - \beta \left(B_{22}^s\alpha_{17} + (B_{12}^s + B_{66}^s)\alpha_{33} + B_{66}^s\alpha_{16} \right) \\ S_{31} &= B_{11}\alpha_{13} + (B_{12} + 2B_{66})\alpha_{11} \\ &\quad - \beta \left(B_{11}^s\alpha_{18} + (B_{12}^s + B_{66}^s)\alpha_{19} + B_{66}^s\alpha_{26} \right) \\ S_{32} &= B_{22}\alpha_5 + (B_{12} + 2B_{66})\alpha_{11} \\ &\quad - \beta \left(B_{22}^s\alpha_{27} + (B_{12}^s + B_{66}^s)\alpha_{26} + B_{66}^s\alpha_{19} \right) \end{aligned} \quad (24)$$

Table 1 The admissible functions $X_m(x)$ and $Y_n(y)$

	Boundary conditions		The functions X_m and Y_n	
	At $x=0,a$	At $y=0, b$	$X_m(x)$	$Y_n(y)$
SSSS	$X_m(0) = X_m''(0) = 0$	$Y_n(0) = Y_n''(0) = 0$	$\sin(\lambda x)$	$\sin(\mu y)$
	$X_m(a) = X_m''(a) = 0$	$Y_n(b) = Y_n''(b) = 0$		
CSSS	$X_m(0) = X_m'(0) = 0$	$Y_n(0) = Y_n''(0) = 0$	$\sin(\lambda x)[\cos(\lambda x) - 1]$	$\sin(\mu y)$
	$X_m(a) = X_m'(a) = 0$	$Y_n(b) = Y_n''(b) = 0$		
CSCS	$X_m(0) = X_m'(0) = 0$	$Y_n(0) = Y_n'(0) = 0$	$\sin(\lambda x)[\cos(\lambda x) - 1]$	$\sin(\mu x)[\cos(\mu x) - 1]$
	$X_m(a) = X_m''(a) = 0$	$Y_n(b) = Y_n''(b) = 0$		
CCSS	$X_m(0) = X_m''(0) = 0$	$Y_n(b) = Y_n''(b) = 0$	$\sin^2(\lambda x)$	$\sin(\mu y)$
	$X_m(a) = X_m''(a) = 0$	$Y_n(b) = Y_n''(b) = 0$		
CCCC	$X_m(0) = X_m'(0) = 0$	$Y_n(0) = Y_n''(0) = 0$	$\sin^2(\lambda x)$	$\sin^2(\mu y)$
	$X_m(a) = X_m'(a) = 0$	$Y_n(b) = Y_n'(b) = 0$		
FFCC	$X_m''(0) = X_m'''(0) = 0$	$Y_n(0) = Y_n'(0) = 0$	$\cos^2(\lambda x)[\sin^2(\lambda x) + 1]$	$\sin^2(\mu y)$
	$X_m''(a) = X_m'''(a) = 0$	$Y_n(b) = Y_n'(b) = 0$		

(\cdot)' Denotes the derivative with respect to the corresponding coordinates

$$\begin{aligned}
 S_{33} = & -D_{11}\alpha_{13} - 2(D_{12} + 2D_{66})\alpha_{11} - D_{22}\alpha_5 - \beta D_{11}^s\alpha_{18} \\
 & - \beta D_{22}^s\alpha_{27} - 2\beta(D_{12}^s + 2D_{66}^s)\alpha_{19} + (D_{12}^s + 2D_{66}^s)\alpha_{26} - \\
 & \beta^2 \left(H_{11}^s\alpha_7 + 2(H_{12}^s + H_{66}^s)\alpha_{21} + H_{66}^s(\alpha_{20} + \alpha_{22}) \right) \\
 & + H_{22}^s\alpha_{23} + A_{44}^s\alpha_{18} + A_{55}^s\alpha_{27} \\
 & + K_{S1}\alpha_9 + K_{S2}\alpha_3 - K_W\alpha_1 - P_x^0\alpha_9 - P_y^0\alpha_3
 \end{aligned} \quad (24)$$

and

$$\begin{aligned}
 m_{11} &= -I_0\alpha_6 \\
 m_{13} &= I_1\alpha_6 + J_1\alpha_{12} \\
 m_{22} &= -I_0\alpha_2 \\
 m_{23} &= I_1\alpha_2 + J_1\alpha_4 \\
 m_{31} &= -I_1\alpha_{31} + \beta J_1\alpha_{13} \\
 m_{32} &= -I_1\alpha_{31} + \beta J_1\alpha_5 \\
 m_{33} &= -I_0\alpha_1 + I_2(\alpha_3 + \alpha_9) + 2\beta J_2(\alpha_{11} + \alpha_5) \\
 &+ \beta^2 K_2(\alpha_{27} + \alpha_{18})
 \end{aligned} \quad (25)$$

with

$$\begin{aligned}
 (\alpha_1, \alpha_3, \alpha_5) &= \int_0^b \int_0^a (X_m Y_m, X_m Y_n'', X_m Y_m^{(IV)}) X_m Y_n dx dy \\
 (\alpha_2, \alpha_4, \alpha_{10}, \alpha_{33}, \alpha_{16}, \alpha_{17}) &= \\
 & \int_0^b \int_0^a (X_m Y_n', X_m Y_n'', X_m Y_n', X_m^{(IV)} Y_n', X_m Y_n'', X_m Y_n^{(V)}) X_m Y_n dx dy \\
 (\alpha_6, \alpha_8, \alpha_{12}) &= \int_0^b \int_0^a (X_m' Y_n, X_m' Y_n'', X_m'' Y_n) X_m' Y_n dx dy \\
 (\alpha_{28}, \alpha_{14}, \alpha_{15}) &= \int_0^b \int_0^a (X_m'' Y_n'', X_m' Y_n^{(IV)}, X_m^{(V)} Y_n) X_m' Y_n dx dy
 \end{aligned} \quad (26)$$

$$(\alpha_7, \alpha_9, \alpha_{11}, \alpha_{13}, \alpha_{18}, \alpha_{19}, \alpha_{20}) = \int_0^b \int_0^a (X_m^{(VIII)} Y_n, X_m'' Y_n, X_m'' Y_n'', X_m^{(IV)} Y_n, X_m^{(VI)} Y_n, X_m'' Y_n^{(IV)}, X_m^{(VI)} Y_n'') X_m Y_n dx dy \quad (26)$$

$$(\alpha_{27}, \alpha_{21}, \alpha_{22}, \alpha_{23}, \alpha_{26}, \alpha_{31}) = \int_0^b \int_0^a (X_m Y_m^{(VI)}, X_m^{(IV)} Y_m^{(IV)}, X_m'' Y_m^{(VI)}, X_m Y_m^{(VIII)}, X_m^{(IV)} Y''', X_m' Y_n) X_m Y_n dx dy$$

The non-trivial solution is determined when the determinant of Eq. (23) equals zero. For the free vibration problem, we have $P_x^0 = P_y^0 = P_{xy}^0 = 0$. While for the buckling analysis, we put $\omega = P_{xy}^0 = 0$; $P_x^0 = \bar{P}$ and $P_y^0 = \xi \bar{P}$, i.e., $\xi = P_y^0 / P_x^0$.

It is noted that the present solution depends on the choice of parameter β of the proposed theory. In this study, the adequate value is taken as a solution of the eigenvalue problem $|S_{ij}| = 0$.

4. Numerical results and discussions

For checking the accuracy of the developed model, several comparisons and parametric studies are presented in the following. All presented results are in dimensionless form as

$$\omega^* = \frac{\omega a^2}{h}; \frac{\bar{P} a^2}{100 h^3}; K_0 = \frac{a^4 K_W}{D}; J_0 = \frac{a^2 K_{S1}}{D} = \frac{b^2 K_{S2}}{D}; D = \frac{h^3 E_c}{12(1-\nu^2)} \quad (27)$$

The properties of the materials used in the FG-sandwich plate are

Ceramic (Alumina, Al_2O_3): $E_c=380$ GPa, $\nu=0.3$, $\rho_c=3800$ kg/m³

Metal (Aluminium, Al): $E_m= 70$ GPa, $\nu=0.3$, $\rho_c=2707$ kg/m³

The configurations (1-0-1, 1-1-1, 1-2-1 and 1-3-1) are

Table 2 Comparison of dimensionless frequency “ ω^* ” of simply supported EGM sandwich square plates “ $k=1.5$ ” resting on Pasternak’s elastic foundations

Scheme	Theory	$K_0 = J_0 = 0$			$K_0 = 100, J_0 = 0$			$K_0 = 100, J_0 = 100$		
		$a/h=5$	$a/h=10$	$a/h=20$	$a/h=5$	$a/h=10$	$a/h=20$	$a/h=5$	$a/h=10$	$a/h=20$
1-0-1	Model 1 _(a)	0.9655	1.0200	1.0356	1.4125	1.4633	1.4781	4.7808	4.8854	4.9135
	Model 2 _(a)	0.9647	1.0198	1.0356	1.4121	1.4632	1.4781	4.7808	4.8854	4.9136
	Present	0.9656	1.0201	1.0357	1.4129	1.4633	1.4782	4.7956	4.8857	4.9136
1-1-1	Model 1 _(a)	1.0811	1.1396	1.1563	1.4697	1.5248	1.5407	4.6537	4.7517	4.7789
	Model 2 _(a)	1.0807	1.1395	1.1563	1.4695	1.5247	1.5407	4.6537	4.7517	4.7789
	Present	1.0812	1.1396	1.1563	1.4700	1.5248	1.5407	4.6629	4.7519	4.7789
1-2-1	Model 1 _(a)	1.1872	1.2578	1.2781	1.5392	1.6045	1.6236	4.6099	4.7076	4.7357
	Model 2 _(a)	1.1872	1.2578	1.2781	1.5392	1.6045	1.6236	4.6100	4.7076	4.7357
	Present	1.1873	1.2578	1.2781	1.5395	1.6045	1.6236	4.6180	4.7078	4.7357
1-3-1	Model 1 _(a)	1.2663	1.3479	1.3716	1.5954	1.6703	1.6924	4.5910	4.6901	4.7192
	Model 2 _(a)	1.2666	1.3480	1.3716	1.5956	1.6704	1.6924	4.5911	4.6901	4.7192
	Present	1.2665	1.3479	1.3716	1.5957	1.6703	1.6924	4.5987	4.6902	4.7192

^(a)Given from Ait Amar Meziane *et al.* (2014)Table 3 Comparison of dimensionless frequency “ ω^* ” of (1-1-1) EGM sandwich plates with various boundary conditions ($b/a=2, K_0=J_0=10$)

B.C	Theory	$k=0$			$k=0.5$			$k=3.5$		
		$a/h=5$	$a/h=10$	$a/h=20$	$a/h=5$	$a/h=10$	$a/h=20$	$a/h=5$	$a/h=10$	$a/h=20$
FFCC	Model 1 _(a)	2.4747	2.8519	2.9944	2.1360	2.3371	2.4055	1.8894	1.9923	2.0248
	Model 2 _(a)	2.4736	2.8516	2.9943	2.1352	2.3368	2.4054	1.8880	1.9918	2.0247
	Present	2.4229	2.7793	2.9660	2.0792	2.2983	2.3926	1.8507	1.9742	2.0194
CCCC	Model 1 _(a)	2.3473	2.6053	2.6953	2.0305	2.1658	2.2093	1.8189	1.8906	1.9124
	Model 2 _(a)	2.3467	2.6052	2.6952	2.0301	2.1657	2.2093	1.8182	1.8904	1.9123
	Present	2.3448	2.6035	2.6947	2.0285	2.1649	2.2091	1.8178	1.8902	1.9123
CSCS	Model 1 _(a)	2.3349	2.5270	2.5906	2.0360	2.1399	2.1722	1.8539	1.9148	1.9328
	Model 2 _(a)	2.3345	2.5269	2.5906	2.0358	2.1398	2.1721	1.8535	1.9146	1.9328
	Present	2.3123	2.5164	2.5875	2.0227	2.1351	2.1708	1.8474	1.9128	1.9323
CCSS	Model 1 _(a)	2.2746	2.5175	2.6015	1.9691	2.0959	2.1364	1.7665	1.8334	1.8536
	Model 2 _(a)	2.2740	2.5173	2.6014	1.9687	2.0957	2.1363	1.7658	1.8331	1.8535
	Present	2.2644	2.5133	2.6003	1.9636	2.0940	2.1358	1.7640	1.8326	1.8534
CSSS	Model 1 _(a)	2.2207	2.3931	2.4496	1.9408	2.0334	2.0619	1.7729	1.8270	1.8429
	Model 2 _(a)	2.2204	2.3930	2.4495	1.9406	2.0334	2.0619	1.7725	1.8269	1.8429
	Present	2.1906	2.3803	2.4458	1.9245	2.0278	2.0604	1.7653	1.8247	1.8423
SSSS	Model 1 _(a)	1.5388	1.5947	1.6113	1.3990	1.4310	1.4401	1.3376	1.3594	1.3655
	Model 2 _(a)	1.5387	1.5948	1.6113	1.3990	1.4310	1.4401	1.3375	1.3594	1.3655
	Present	1.5438	1.5963	1.6117	1.4010	1.4316	1.4403	1.3384	1.3597	1.3655

^(a)Given from Ait Amar Meziane *et al.* (2014)

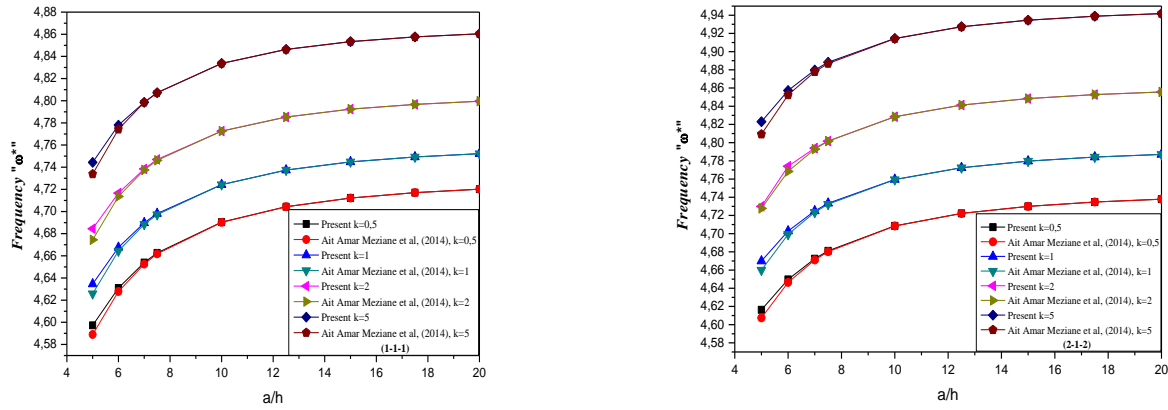


Fig. 2 Dimensionless frequency " ω^* " versus the ratio " a/h " for various values of the inhomogeneity parameter " k " and various types of simply- supported EGM sandwich square plates resting on elastic foundations " $K_0=J_0=100$ "

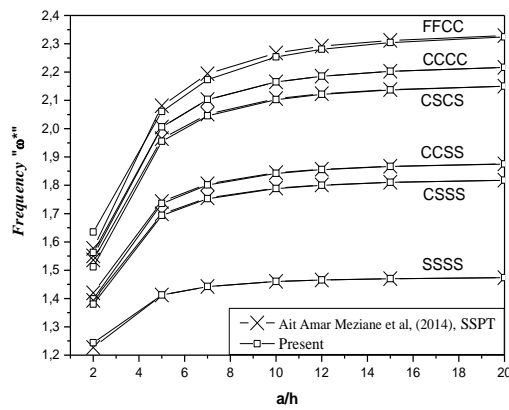


Fig. 3 Dimensionless frequency " ω^* " versus the ratio " a/h " of the (2-1-2) E-FG sandwich square plates resting on Winkler's elastic foundation with various boundary conditions ($K_0=100, k=2$)

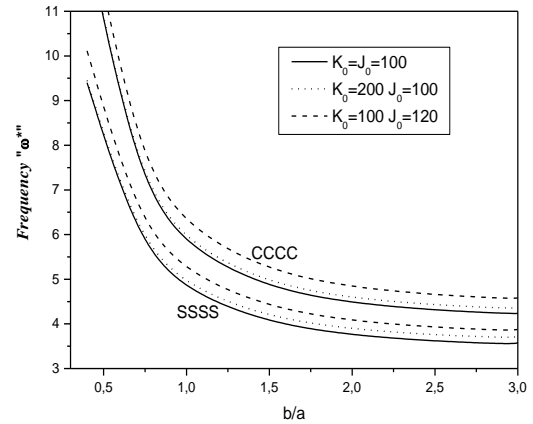


Fig. 4 Dimensionless frequency " ω^* " versus the aspect ratio " b/a " of simply-supported and clamped E-FG sandwich plate (1-2-1) for different values of foundation stiffness's " K_0 " and " J_0 " ($a/h=10, k=2$)

the layers thicknesses ratio defined as

- 1-0-1 the plate is made of two layers of equal thickness without a core.
- 1-1-1 the plate has the same thicknesses of the layers (core and faces sheets)
- 1-2-1 the plate has the thickness of the core is twice the thickness of face sheets.
- 1-3-1 the plate has the thickness of the core is thrice the thickness of face sheets.

4.1 Free vibration of the FG sandwich plate

In this first part, several numerical results of the free vibrational analysis of the FG-sandwich plate with and without elastic foundation computed by the current three unknowns shear deformation theory are presented in the form of explicit tables and graphs.

To verify the accuracy of the current model, the obtained results of the free vibrational analysis of the simply supported E-FG sandwich plate resting on elastic foundations are compared with the models existing in the literature (Ait Amar Meziane *et al.* 2014). From the results of the fundamental frequency of the E-FG sandwich plate are given in the Table 2, it can be seen that the present model is in good agreement with the two models developed

by Ait Amar Meziane *et al.* (2014). We can note from the results that the thick E-FG sandwich plate give the smaller value of the fundamental frequencies. Also, it is clear that the configuration 1-3-1 give the biggest values of the fundamental frequency.

The Table 3 shows the comparison of the fundamental frequency " ω^* " of the (1-1-1) rectangular E-FG sandwich plate on the Winkler-Pasternak elastic foundation " $J_1=J_2=10$ " versus the material index " k " and geometry ratio " a/h " with various boundary conditions (FFCC, CCCC, CSCS, CCSS, CSSS and SSSS). From the comparison made in the Table 3, it is clear that the current results obtained using the present three unknowns shear deformation theory are in good agreement those computed by Ait Amar Meziane *et al.* (2014) with four variable refined shear deformation model.

From the table, we can see that the increasing in the values of the material index " k " lead to decrease the fundamental frequencies " ω^* " for different boundary conditions.

It can be also concluded that the FG sandwich plate with two free edges and two opposite clamped edges (FFCC) give the biggest values of the frequency " ω^* "

The variation of the non-dimensional fundamental

Table 4 Comparison of critical buckling load “ \bar{N} ” of simply supported EGM sandwich square plates “ $k=0.5$ ” resting on Pasternak’s elastic foundations “ $\zeta=1$ ”

Scheme	Theory	$K_0=J_0=0$			$K_0=100, J_0=0$			$K_0=100, J_0=100$		
		$a/h=5$	$a/h=10$	$a/h=20$	$a/h=5$	$a/h=10$	$a/h=20$	$a/h=5$	$a/h=10$	$a/h=20$
1-0-1	Model 1 ^(a)	2.5618	2.8127	2.8834	4.3247	4.5756	4.6463	39.1232	39.3741	39.4449
	Model 2 ^(a)	2.5592	2.8120	2.8833	4.3221	4.5749	4.6462	39.1206	39.3734	39.4447
	Present	2.5618	2.8127	2.8835	4.3247	4.5757	4.6464	39.1233	39.3742	39.4449
1-1-1	Model 1 ^(a)	3.1030	3.4156	3.5040	4.8659	5.1785	5.2669	39.6644	39.9770	40.0655
	Model 2 ^(a)	3.1015	3.4152	3.5039	4.8644	5.1781	5.2668	39.6629	39.9766	40.0654
	Present	3.1030	3.4156	3.5040	4.8659	5.1785	5.2670	39.6645	39.9771	40.0655
1-2-1	Model 1 ^(a)	3.5165	3.9026	4.0129	5.2795	5.6655	5.7758	40.0780	40.4640	40.5744
	Model 2 ^(a)	3.5166	3.9027	4.0130	5.2795	5.6656	5.7759	40.0780	40.4641	40.5744
	Present	3.5166	3.9026	4.0129	5.2795	5.6655	5.7759	40.0780	40.4641	40.5744
1-3-1	Model 1 ^(a)	3.8243	4.2743	4.4030	5.5872	6.0364	6.1659	40.3857	40.8349	40.9644
	Model 2 ^(a)	3.8253	4.2738	4.4031	5.5882	6.0368	6.1660	40.3868	40.8353	40.9646
	Present	3.8243	4.2735	4.4030	5.5872	6.0364	6.1659	40.3858	40.8349	40.9645

^(a) Given from Ait Amar Meziane *et al.* (2014)Table 5 Comparison of critical buckling load “ \bar{N} ” of (1-1-1) EGM sandwich plates with various boundary conditions ($b/a=2, K_0=J_0=10$)

B.C	Theory	$k=0$			$k=0.5$			$k=3.5$		
		$a/h=5$	$a/h=10$	$a/h=20$	$a/h=5$	$a/h=10$	$a/h=20$	$a/h=5$	$a/h=10$	$a/h=20$
FFCC	Model 1 ^(a)	15.7316	20.6940	22.6679	10.9709	12.9380	13.6121	7.8557	8.5665	8.7850
	Model 2 ^(a)	15.7165	20.6896	22.6667	10.9609	12.9346	13.6112	7.8423	8.5621	8.7838
	Present	15.2671	19.6685	22.2406	10.4701	12.5168	13.4665	7.5660	8.4128	8.7379
CCCC	Model 1 ^(a)	13.0716	15.8553	16.8365	9.1520	10.1974	10.5257	6.7161	7.0785	7.1835
	Model 2 ^(a)	13.0640	15.8532	16.8360	9.1467	10.1958	10.5252	6.7091	7.0764	7.1829
	Present	13.0641	15.8351	16.8293	9.1407	10.1897	10.5233	6.7099	7.0759	7.1827
CSCS	Model 1 ^(a)	10.9052	12.4673	12.9712	7.7552	8.3183	8.4846	5.8764	6.0659	6.1185
	Model 2 ^(a)	10.9012	12.4662	12.9709	7.7523	8.3175	8.4843	5.8726	6.0648	6.1182
	Present	10.7534	12.3673	12.9397	7.6747	8.2825	8.4742	5.8427	6.0539	6.1152
CCSS	Model 1 ^(a)	12.9080	15.5750	16.5080	9.0485	10.0467	10.3584	6.6581	7.0033	7.1028
	Model 2 ^(a)	12.9010	15.5729	16.5074	9.0435	10.0451	10.3580	6.6514	7.0013	7.1023
	Present	12.8160	15.5259	16.4928	9.0059	10.0293	10.3535	6.6412	6.9975	7.1013
CSSS	Model 1 ^(a)	10.6425	12.0761	12.5336	7.5981	8.1123	8.2630	5.7919	5.9643	6.0120
	Model 2 ^(a)	10.6389	12.0752	12.5334	7.5955	8.1116	8.2628	5.7885	5.9633	6.0117
	Present	10.4029	11.9501	12.4954	7.4871	8.0681	8.2505	5.7483	5.9497	6.0080
SSSS	Model 1 ^(a)	7.5261	7.9091	8.0175	5.7942	5.9239	5.9590	4.8267	4.8685	4.8795
	Model 2 ^(a)	7.5253	7.9089	8.0175	5.7936	5.9238	5.9590	4.8259	4.8684	4.8795
	Present	7.5804	7.9249	8.0217	5.8129	5.9291	5.9604	4.8328	4.8702	4.8799

^(a) Given from Ait Amar Meziane *et al.* (2014)

frequencies “ ω^* ” of simply supported E-FG sandwich plate on elastic foundations versus geometry ratio “ a/h ” and index “ k ” are plotted in the Fig. 2. The aspect ratio is taken

“ $a/b=1$ ”. From the graphs it can be seen that the non-dimensional fundamental frequencies “ ω^* ” is in direct correlation relation with the both the index “ k ” and “ a/h ”

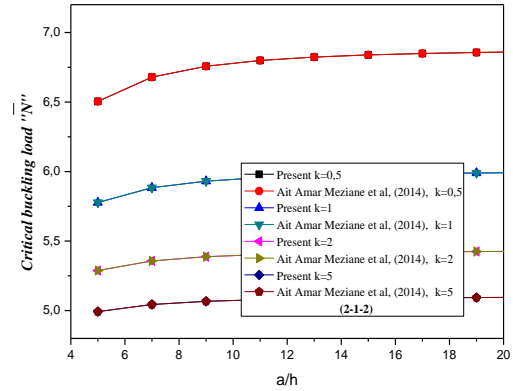
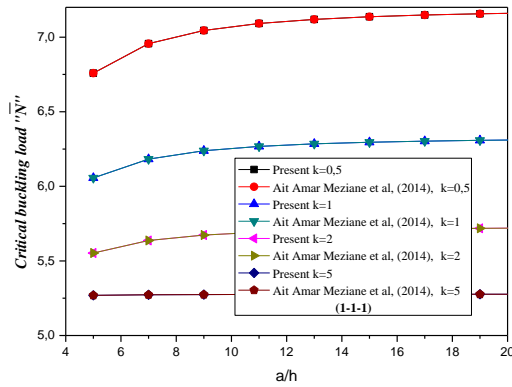


Fig. 5 Critical buckling load " \bar{N} " versus the ratio " a/h " for various values of the inhomogeneity parameter " k " and various types of simply- supported EGM sandwich square plates resting on elastic foundations($K_0=J_0=10$, $\xi=1$, $a=b$)

ratio and this is the same for the 1-1-1 and 2-1-2 FG plate. It can be confirmed again that the results are in good agreement with those given in the literature (Ait Amar Meziane *et al.* 2014).

Fig. 3 plot the non-dimensional frequency " ω^* " of 2-1-2 FG-sandwich plate on elastic foundations with " $K_0=100$, $k=2$ " versus the type of boundary conditions and geometry ratio " a/h ". The obtained results are compared with those given by Ait Amar Meziane *et al.* (2014). A good agreement is confirmed between current results and those computed by Ait Amar Meziane *et al.* (2014). From the plotted curves it can be noted that the boundary condition has an important role on the non-dimensional frequency " ω^* " it is clear from the graphs that the biggest values of the non-dimensional frequency " ω^* " are obtained for FFCC FG-sandwich plate. It is confirmed again that the non-dimensional frequency " ω^* " increase with increasing in the values of the " a/h ".

Fig. 4 gives the variation of the frequencies " ω^* " versus the aspect ratio b/a , boundary conditions and foundations parameters " K_0, J_0 " of the 1-2-1 E-FG sandwich plate with " $a/h=10$, $k=2$ ". From the plotted graphs, we can see clearly that the FG-plate with four clamped edges gives the bigger values of the frequencies " ω^* " than simply supported FG-plate. It can be observed also that the smaller values of the frequency " ω^* " are obtained of the plate with foundations parameters ($K_0, J_0=100$). Also an inverse relation is observed between the aspect ratio and frequency " ω^* ".

4.2 Stability of the FG sandwich plate

The second part is reserved to numerical results of the buckling analysis of the E-FG sandwich plate with and without elastic foundation with various boundary conditions.

Table 4 present a comparison of the critical buckling load " \bar{N} " of simply supported E-FG sandwich square plates " $k=0.5$ " reposed on Winkler-Pasternak elastic foundations. From the computed results, it can be seen that the current model is in good agreement with those obtained by Ait Amar Meziane *et al.* (2014) for various type of simply supported FG-sandwich plate (1-0-1, 1-1-1, 1-2-1 and 1-3-1). It can be observed from the results that the presence of the Winkler-Pasternak elastic foundations lead to an increase of the critical buckling load of the FG-sandwich

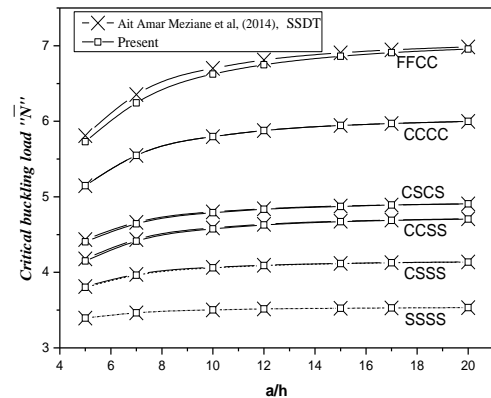


Fig. 6 Critical buckling load " \bar{N} " versus the ratio " a/h " of the (2-1-2) EGM sandwich square plates resting on Winkler's elastic foundation with various boundary conditions ($K_0=100$, $k=2$, $\xi=1$)

plate. From the comparison of the various types of the FG-sandwich plate, it is clear that the 1-3-1 FG-plate gives the higher values of the critical buckling load.

Table 5 shows the comparison of the critical buckling load " \bar{N} " of the (1-1-1) rectangular E-FG sandwich plate on the elastic foundation " $K_0=J_0=10$ " as function the parameters " k " and " a/h " with different boundary conditions (FFCC, CCCC, CSCS, CCSS, CSSS and SSSS). From the table, it is can be confirmed again that the present model with only three unknown give almost the same results of the critical buckling load " \bar{N} " of FG-sandwich plate as those computed by Ait Amar Meziane *et al.* (2014) with RPT model. From the results, we can observe that the critical buckling load " \bar{N} " is in inverse relation with the material index " k " for various boundary conditions. It can be also concluded that the smaller values of the critical buckling load " \bar{N} " are given by a simply-supported FG-sandwich plate.

The critical buckling load " \bar{N} " versus the ratio " a/h " and inhomogeneity parameter " k " of simply- supported E-FG sandwich plates seated on elastic foundations with ($K_0=J_0=10$, $\xi=1$, $a=b$) is illustrated in Fig. 5. From the plotted curves, it can be noted that the current results are almost the same with those given by Ait Amar Meziane *et al.* (2014). It can also be observed that the increasing in the ratio " a/h " leads to an increase in the critical buckling

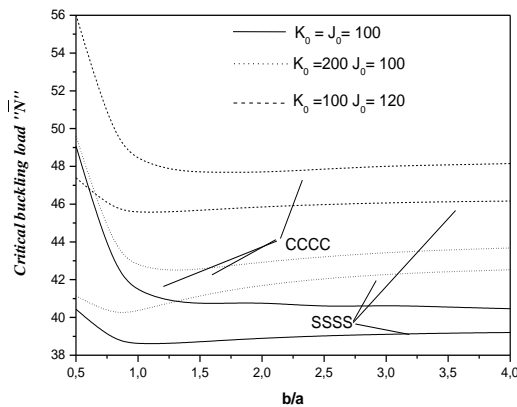


Fig. 7 Critical buckling load " \bar{N} " versus the aspect ratio " b/a " of simply-supported and clamped E-FG sandwich plate (1-1-1) for different values of foundation stiffness's " K_0 " and " J_0 " ($a/h=10, k=2, \zeta=1$)

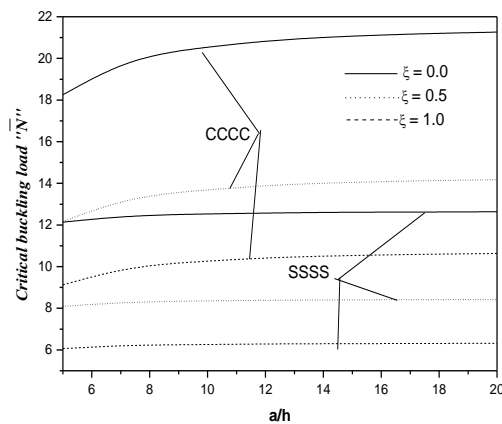


Fig. 8 Critical buckling load " \bar{N} " versus the ratio " a/h " of simply-supported and clamped E-FG sandwich square plate (1-2-1) for different values of " ζ " ($K_0=J_0=10, k=2$)

load " \bar{N} ". But this last decreases when the inhomogeneity parameter " k " increases.

Fig. 6 illustrates the variation of critical buckling load " \bar{N} " of the 2-1-2 FG-sandwich plate seated elastic foundation with ($K_0=100, k=2$) for various boundary conditions (FFCC, CCCC, CSCS, CCSS, CSSS and SSSS). The FG sandwich plate is supposed under biaxial compressive loads " $\zeta=1$ ".

The present results of the critical buckling load " \bar{N} " are in good agreement with those given by Ait Amar Meziane *et al.* (2014). From the graphs it can be observed that smaller values of the critical buckling load " \bar{N} " are obtained for SSSS FG-sandwich plate.

Fig. 7 presents the variation of the critical buckling load " \bar{N} " of the clamped and simply supported 1-1-1 E-FG sandwich plate with ($a/h=10, k=2$) as foundations parameters " K_0, J_0 ". From the obtained graphs, it can be noted that the biggest values of the critical buckling load " \bar{N} " are obtained for parameters " $K_0=100, J_0=120$ " and this is confirmed for both SSSS and CCCC boundary conditions.

The variations of the critical buckling load " \bar{N} " of the 1-

2-1 FG-sandwich plate on elastic foundation versus loads ratio " ζ " are illustrated in the Fig. 8. From the plotted curves, it can be noted that the smaller values of the critical buckling load " \bar{N} " are obtained for simply supported E-FG with biaxial compressive load " $\zeta=1$ ". But the larger values are obtained for clamped FG-sandwich plate under uniaxial compressive load along x-axis.

5. Conclusions

A simplified innovative trigonometric higher orders shear deformation with only three unknowns variable was developed for free vibrational and mechanical stability analysis of E-FG sandwich plate with various boundary conditions. The equations of motion are obtained from the Hamilton's principle. The accuracy and efficiency of the developed model has been checked for the stability and dynamic analysis of FG-sandwich plate. Several parametric studies has been examined and discussed to show the various parameters influencing the fundamental frequency and critical buckling load of the plate.

Finally it can be concluded that, the present theory can improve the numerical computational cost due to their reduced degrees of freedom and it can be used to study other structures made of different types of materials (Sedighi and Shirazi 2013, Avcar 2014 Sedighi *et al.* 2015, Panjehpour *et al.* 2018, Othman and Fekry 2018, Dihaj *et al.* 2018, Belmahi, *et al.* 2018, Yaylacl *et al.* 2019, Al-Maliki *et al.* 2020, López-Chavarría *et al.* 2019, Nikkhoo *et al.* 2019, Kossakowski and Uzarska 2019, Zouatnia and Hadji 2019, Bakhshi and Taheri-Behrooz 2019, Belmahi *et al.* 2019, Fládr *et al.* 2019, Hamad *et al.* 2019, Mohamed *et al.* 2019, Jothi Saravanan *et al.* 2019, Khater *et al.* 2020, Singh and Kumari 2020, Rezaiee-Pajand and Karimipour 2020, Ghadimi 2020, Shokrieh and Kondori 2020, Ghannadpour and Mehrparvar 2020, Lee *et al.* 2020, Yüksel and Akbaş 2019, Karami and Janghorban 2019, Selmi 2019, Al-Basyouni *et al.* 2020, Safarpour *et al.* 2020, Kunche *et al.* 2019, Eltaher *et al.* 2020, Motezaker *et al.* 2020, Ghabussi *et al.* 2020, Timesli 2020).

References

- Abdelmalek, A., Bouazza, M., Zidour, M. and Benseddig, N. (2019), "Hygrothermal effects on the free vibration behavior of composite plate using nth-order shear deformation theory: A micromechanical approach", *Iran. J. Sci. Technol. Trans. Mech. Eng.*, **43**, 61-73. <https://doi.org/10.1007/s40997-017-0140-y>.
- Abdulrazzaq, M.A., Fenjan, R.M., Ahmed, R.A. and Faleh, N.M. (2020), "Thermal buckling of nonlocal clamped exponentially graded plate according to a secant function based refined theory", *Steel Compos. Struct.*, **35**(1), 147-157. <https://doi.org/10.12989/scs.2020.35.1.147>.
- Adim, B., Daouadji, T.H. and Rabahi, A. (2016), "A simple higher order shear deformation theory for mechanical behavior of laminated composite plates", *Int. J. Adv. Struct. Eng.*, **8**(2), 103-117. <https://doi.org/10.1007/s40091-016-0109-x>.
- Ahmed, R.A., Fenjan, R.M. and Faleh, N.M. (2019), "Analyzing post-buckling behavior of continuously graded FG nanobeams with geometrical imperfections", *Geomech. Eng.*, **17**(2), 175-

180. <https://doi.org/10.12989/gae.2019.17.2.175>.
- Ait Amar Meziane, M., Abdelaziz, H.H. and Tounsi, A. (2014), "An efficient and simple refined theory for buckling and free vibration of exponentially graded sandwich plates under various boundary conditions", *J. Sandw. Struct. Mater.*, **16**(3), 293-318. <https://doi.org/10.1177/1099636214526852>.
- Akgoz, B. and Civalek, O. (2011), "Nonlinear vibration analysis of laminated plates resting on nonlinear two-parameters elastic foundations", *Steel Compos. Struct.*, **11**(5), 403-421. <https://doi.org/10.12989/scs.2011.11.5.403>.
- Al-Basyouni, K.S., Ghandourah, E., Mostafa, H.M. and Algarni, A. (2020), "Effect of the rotation on the thermal stress wave propagation in non-homogeneous viscoelastic body", *Geomech. Eng.*, **21**(1), 1-9. <https://doi.org/10.12989/gae.2020.21.1.001>.
- Al-Maliki, A.F.H., Ahmed, R.A., Moustafa, N.M. and Faleh, N.M. (2020), "Finite element based modeling and thermal dynamic analysis of functionally graded graphene reinforced beams", *Adv. Comput. Des.*, **5**(2), 177-193. <https://doi.org/10.12989/acd.2020.5.2.177>.
- Avcar, M. (2014), "Free vibration analysis of beams considering different geometric characteristics and boundary conditions", *Int. J. Mech. Appl.*, **4**(3), 94-100. <https://doi.org/10.5923/j.mechanics.20140403.03>.
- Avcar, M. (2016), "Effects of material non-homogeneity and two parameter elastic foundation on fundamental frequency parameters of Timoshenko beams", *Acta Physica Polonica A*, **130**(1), 375-378. <https://doi.org/10.12693/APhysPolA.130.375>.
- Avcar, M. (2019), "Free vibration of imperfect sigmoid and power law functionally graded beams", *Steel Compos. Struct.*, **30**(6), 603-615. <https://doi.org/10.12989/scs.2019.30.6.603>.
- Avcar, M. and Mohammed, W.K.M. (2018), "Free vibration of functionally graded beams resting on Winkler-Pasternak foundation", *Arab. J. Geosci.*, **11**(10), 232. <https://doi.org/10.1007/s12517-018-3579-2>.
- Bakhshi, N. and Taheri-Behrooz, F. (2019), "Length effect on the stress concentration factor of a perforated orthotropic composite plate under in-plane loading", *Compos. Mater. Eng.*, **1**(1), 71-90. <https://doi.org/10.12989/cme.2019.1.1.071>.
- Belmahi, S., Zidour, M. and Meradjah, M. (2019), "Small-scale effect on the forced vibration of a nano beam embedded an elastic medium using nonlocal elasticity theory", *Adv. Aircraft Spacecraft Sci.*, **6**(1), 1-18. <https://doi.org/10.12989/aas.2019.6.1.001>.
- Belmahi, S., Zidour, M., Meradjah, M., Bensattallah, T. and Dihaj, A. (2018), "Analysis of boundary conditions effects on vibration of nanobeam in a polymeric matrix", *Struct. Eng. Mech.*, **67**(5), 517-525. <https://doi.org/10.12989/sem.2018.67.5.517>.
- Bensattallah, T., Zidour, M. and Daouadji, T.H. (2019), "A new nonlocal beam model for free vibration analysis of chiral single-walled carbon nanotubes", *Compos. Mater. Eng.*, **1**(1), 21-31. <https://doi.org/10.12989/cme.2019.1.1.021>.
- Civalek, Ö. and Acar, M.H. (2007), "Discrete singular convolution method for the analysis of Mindlin plates on elastic foundations", *Int. J. Pressure Vessels Piping*, **84**(9), 527-535. <https://doi.org/10.1016/j.ijpvp.2007.07.001>.
- Dash, S., Mehar, K., Sharma, N., Mahapatra, T.R. and Panda, S.K. (2018), "Modal analysis of FG sandwich doubly curved shell structure", *Struct. Eng. Mech.*, **68**(6), 721-733. <https://doi.org/10.12989/sem.2018.68.6.721>.
- Dihaj, A., Zidour, M., Meradjah, M., Rakrak, K., Heireche, H. and Chemi, A. (2018), "Free vibration analysis of chiral double-walled carbon nanotube embedded in an elastic medium using non-local elasticity theory and Euler Bernoulli beam model", *Struct. Eng. Mech.*, **65**(3), 335-342. <https://doi.org/10.12989/sem.2018.65.3.335>.
- Ebrahimi, F. and Barati, M.R. (2017a), "Buckling analysis of nonlocal strain gradient axially functionally graded nanobeams resting on variable elastic medium", *Proc. Inst. Mech. Eng. Part C J. Mech. Eng. Sci.*, **232**(11), 2067-2078. <https://doi.org/10.1177/0954406217713518>.
- Eltaher, M.A. and Mohamed, S.A. (2020), "Buckling and stability analysis of sandwich beams subjected to varying axial loads", *Steel Compos. Struct.*, **34**(2), 241-260. <https://doi.org/10.12989/scs.2020.34.2.241>.
- Eltaher, M.A., Mohamed, S.A. and Melaibari, A. (2020), "Static stability of a unified composite beams under varying axial loads", *Thin Walled Struct.*, **147**, 106488. <https://doi.org/10.1016/j.tws.2019.106488>.
- Eltaher, M.A., Agwa, M. and Kabeel, A. (2018), "Vibration analysis of material size-dependent CNTs using energy equivalent model", *J. Appl. Comput. Mech.*, **4**(2), 75-86. <https://doi.org/10.22055/JACM.2017.22579.1136>.
- Fenjan, R.M., Ahmed, R.A., Alasadi, A.A. and Faleh, N.M. (2019a), "Nonlocal strain gradient thermal vibration analysis of double-coupled metal foam plate system with uniform and non-uniform porosities", *Coupled Syst. Mech.*, **8**(3), 247-257. <https://doi.org/10.12989/csm.2019.8.3.247>.
- Fenjan, R.M., Ahmed, R.A. and Faleh, N.M. (2019b), "Investigating dynamic stability of metal foam nanoplates under periodic in-plane loads via a three-unknown plate theory", *Adv. Aircraft Spacecraft Sci.*, **6**(4), 297-314. <https://doi.org/10.12989/aas.2019.6.4.297>.
- Fládr, J., Bílý, P. and Broukalová, I. (2019), "Evaluation of steel fiber distribution in concrete by computer aided image analysis", *Compos. Mater. Eng.*, **1**(1), 49-70. <https://doi.org/10.12989/cme.2019.1.1.049>.
- Ghabussi, A., Habibi, M., Arani, O.N., Shavalipour, A., Moayedi, H. and Safarpour, H. (2020), "Frequency characteristics of a viscoelastic graphene nanoplatelet-reinforced composite circular microplate", *J. Vib. Control*, In Press. <https://doi.org/10.1177/1077546320923930>.
- Ghadimi, M.G. (2020), "Buckling of non-sway Euler composite frame with semi-rigid connection", *Compos. Mater. Eng.*, **2**(1), 13-24. <https://doi.org/10.12989/cme.2020.2.1.013>.
- Ghannadpour, S.A.M. and Mehrparvar, M. (2020), "Modeling and evaluation of rectangular hole effect on nonlinear behavior of imperfect composite plates by an effective simulation technique", *Compos. Mater. Eng.*, **2**(1), 25-41. <https://doi.org/10.12989/cme.2020.2.1.025>.
- Ghugal, Y.M. and Sayyad, A.S. (2011), "Free vibration of thick orthotropic plates using trigonometric shear deformation theory", *Lat. Amer. J. Solids Struct.*, **8**(3), 229-243. <https://doi.org/10.1590/s1679-78252011000300002>.
- Hadji, L., Zouatnia, N. and Bernard, F. (2019), "An analytical solution for bending and free vibration responses of functionally graded beams with porosities: Effect of the micromechanical models", *Struct. Eng. Mech.*, **69**(2), 231-241. <https://doi.org/10.12989/sem.2019.69.2.231>.
- Hamad, L.B., Khalaf, B.S. and Faleh, N.M. (2019), "Analysis of static and dynamic characteristics of strain gradient shell structures made of porous nano-crystalline materials", *Adv. Mater. Res.*, **8**(3), 179-196. <https://doi.org/10.12989/amr.2019.8.3.179>.
- Hamed, M.A., Mohamed, S.A. and Eltaher, M.A. (2020), "Buckling analysis of sandwich beam rested on elastic foundation and subjected to varying axial in-plane loads", *Steel Compos. Struct.*, **34**(1), 75-89. <https://doi.org/10.12989/scs.2020.34.1.075>.
- Hamidi, A., Zidour, M., Bouakkaz, K. and Bensattallah, T. (2018), "Thermal and small-scale effects on vibration of embedded armchair single-walled carbon nanotubes", *J. Nano Res.*, **51**, 24-38. <https://doi.org/10.4028/www.scientific.net/JNanoR.51.24>.
- Jothi Saravanan, T., Gopalakrishnan, N. and Karthick Hari, B.

- (2019), "Damage identification in structural elements through curvature mode shapes and nonlinear energy operator", *Compos. Mater. Eng.*, **1**(1), 33-48.
<https://doi.org/10.12989/cme.2019.1.1.033>.
- Kar, V.R. and Panda, S.K. (2015), "Nonlinear flexural vibration of shear deformable functionally graded spherical shell panel", *Steel Compos. Struct.*, **18**(3), 693-709.
<https://doi.org/10.12989/scs.2015.18.3.693>.
- Kar, V.R. and Panda, S.K. (2017), "Large-amplitude vibration of functionally graded doubly-curved panels under heat conduction", *AIAA J.*, **55**(12), 4376-4386.
<https://doi.org/10.2514/1.J055878>.
- Karama, M., Afaq, K.S. and Mistou, S. (2003), "Mechanical behaviour of laminated composite beam by the new multi-layered laminated composite structures model with transverse shear stress continuity", *Int. J. Solids Struct.*, **40**(6), 1525-1546.
[https://doi.org/10.1016/S0020-7683\(02\)00647-9](https://doi.org/10.1016/S0020-7683(02)00647-9).
- Karami, B., Shahsavari, D. and Janghorban, M. (2019), "On the dynamics of porous doubly-curved nanoshells", *Int. J. Eng. Sci.*, **143**, 39-55. <https://doi.org/10.1016/j.ijengsci.2019.06.014>.
- Karami, B. and Janghorban, M. (2019), "On the dynamics of porous nanotubes with variable material properties and variable thickness", *Int. J. Eng. Sci.*, **136**, 53-66.
<https://doi.org/10.1016/j.ijengsci.2019.01.002>.
- Katariya, P.V. and Panda, S.K. (2016), "Thermal buckling and vibration analysis of laminated composite curved shell panel", *Aircr. Eng. Aerosp. Technol.*, **88**(1), 97-107.
<https://doi.org/10.1108/AEAT-11-2013-0202>.
- Katariya, P.V. and Panda, S.K. (2019a), "Frequency and deflection responses of shear deformable skew sandwich curved shell panel: A finite element approach", *Arab. J. Sci. Eng.*, **44**, 1631-1648. <https://doi.org/10.1007/s13369-018-3633-0>.
- Katariya, P.V. and Panda, S.K. (2019b), "Numerical frequency analysis of skew sandwich layered composite shell structures under thermal environment including shear deformation effects", *Struct. Eng. Mech.*, **71**(6), 657-668.
<https://doi.org/10.12989/sem.2019.71.6.657>.
- Katariya, P.V. and Panda, S.K. (2020), "Numerical analysis of thermal post-buckling strength of laminated skew sandwich composite shell panel structure including stretching effect", *Steel Compos. Struct.*, **34**(2), 279-288.
<https://doi.org/10.12989/scs.2020.34.2.279>.
- Katariya, P.V., Panda, S.K., Hirwani, C.K., Mehar, K. and Thakare, O. (2017), "Enhancement of thermal buckling strength of laminated sandwich composite panel structure embedded with shape memory alloy fibre", *Smart Struct. Syst.*, **20**(5), 595-605. <https://doi.org/10.12989/sss.2017.20.5.595>.
- Katariya, P.V., Panda, S.K. and Mahapatra, T.R. (2018), "Bending and vibration analysis of skew sandwich plate", *Aircr. Eng. Aerosp. Technol.*, **90**(6). <https://doi.org/10.1108/AEAT-05-2016-0087>.
- Katariya, P.V., Panda, S.K. and Mahapatra, T.R. (2019), "Prediction of nonlinear eigenfrequency of laminated curved sandwich structure using higher-order equivalent single-layer theory", *J. Sandw. Struct. Mater.*, **21**(8), 2846-2869.
<https://doi.org/10.1177/1099636217728420>.
- Khater, H.M., El Nagar, A.M., Ezzat, M. and Lottfy, M. (2020), "Fabrication of sustainable geopolymer mortar incorporating granite waste", *Compos. Mater. Eng.*, **2**(1), 1-12.
<https://doi.org/10.12989/cme.2020.2.1.001>.
- Kirlangic, O. and Akbaş, Ş.D. (2020), "Comparison study between layered and functionally graded composite beams for static deflection and stress analyses", *J. Comput. Appl. Mech.*, <https://doi.org/10.22059/JCAMECH.2020.296319.473>.
- Kossakowski, P.G. and Uzarska, I. (2019), "Numerical modeling of an orthotropic RC slab band system using the Barcelona model", *Adv. Comput. Des.*, **4**(3), 211-221.
<https://doi.org/10.12989/acd.2019.4.3.211>.
- Kunche, M.C., Mishra, P.K., Nallala, H.B., Hirwani, C.K., Katariya, P.V., Panda, S. and Panda, S.K. (2019), "Theoretical and experimental modal responses of adhesive bonded T-joints", *Wind Struct.*, **29**(5), 361-369.
<https://doi.org/10.12989/was.2019.29.5.361>.
- Lee, N.J., Lai, G.S., Lau, W.J. and Ismail, A.F. (2020), "Effect of poly(ethylene glycol) on the properties of mixed matrix membranes for improved filtration of highly concentrated oily solution", *Compos. Mater. Eng.*, **2**(1), 43-51.
<https://doi.org/10.12989/cme.2020.2.1.043>.
- López-Chavarría, S., Luévanos-Rojas, A., Medina-Elizondo, M., Sandoval-Rivas, R. and Velázquez-Santillán, F. (2019), "Optimal design for the reinforced concrete circular isolated footings", *Adv. Comput. Des.*, **4**(3), 273-294.
<https://doi.org/10.12989/acd.2019.4.3.273>.
- Malekzadeh, P. and Monajjemzadeh, S.M. (2013), "Dynamic response of functionally graded plates in thermal environment under moving load", *Compos. Part B Eng.*, **45**(1), 1521-1533.
<https://doi.org/10.1016/j.compositesb.2012.09.022>.
- Mehar, K. and Panda, S.K. (2018), "Thermal free vibration behavior of FG-CNT reinforced sandwich curved panel using finite element method", *Polym. Compos.*, **39**(8), 2751-2764.
<https://doi.org/10.1002/pc.24266>.
- Mehar, K. and Panda, S.K. (2019), "Multiscale modeling approach for thermal buckling analysis of nanocomposite curved structure", *Adv. Nano Res.*, **7**(3), 181-190.
<https://doi.org/10.12989/anr.2019.7.3.181>.
- Mehar, K., Panda, S.K., Dehengia, A. and Kar, V.R. (2016), "Vibration analysis of functionally graded carbon nanotube reinforced composite plate in thermal environment", *J. Sandw. Struct. Mater.*, **18**(2), 151-173.
<https://doi.org/10.1177/1099636215613324>.
- Mehar, K., Panda, S.K., Devarajan, Y. and Choubey, G. (2019), "Numerical buckling analysis of graded CNT-reinforced composite sandwich shell structure under thermal loading", *Compos. Struct.*, **240**, 112064.
<https://doi.org/10.1016/j.compstruct.2019.03.002>.
- Mehar, K., Panda, S.K. and Mahapatra, T.R. (2017), "Theoretical and experimental investigation of vibration characteristic of carbon nanotube reinforced polymer composite structure", *Int. J. Mech. Sci.*, **133**, 319-329.
<https://doi.org/10.1016/j.ijmecsci.2017.08.057>.
- Mehar, K., Panda, S.K. and Sharma, N. (2020), "Numerical investigation and experimental verification of thermal frequency of carbon nanotube-reinforced sandwich structure", *Eng. Struct.*, **211**, 110444.
<https://doi.org/10.1016/j.engstruct.2020.110444>.
- Mirjavadi, S.S., Forsat, M., Barati, M.R., Abdella, G.M., Mohasel Afshari, B., Hamouda, A.M.S. and Rabby, S. (2019a), "Dynamic response of metal foam FG porous cylindrical micro-shells due to moving loads with strain gradient size-dependency", *Eur. Phys. J. Plus*, **134**(5).
<https://doi.org/10.1140/epjp/i2019-12540-3>.
- Mirjavadi, S.S., Forsat, M., Nikookar, M., Barati, M.R. and Hamouda, A.M.S. (2019b), "Nonlinear forced vibrations of sandwich smart nanobeams with two-phase piezo-magnetic face sheets", *Eur. Phys. J. Plus*, **134**, 508.
<https://doi.org/10.1140/epjp/i2019-12806-8>.
- Mohamed, N., Mohamed A. Eltaher, M.A., Mohamed, S.A and Seddek, L.F. (2019), "Energy equivalent model in analysis of postbuckling of imperfect carbon nanotubes resting on nonlinear elastic foundation", *Struct. Eng. Mech.*, **70**(6), 737-750. <https://doi.org/10.12989/sem.2019.70.6.737>.
- Motezaker, M., Jamali, M. and Kolahchi, R. (2020), "Application of differential cubature method for nonlocal vibration, buckling and bending response of annular nanoplates integrated by

- piezoelectric layers based on surface-higher order nonlocal-piezoelectricity theory", *J. Comput. Appl. Math.*, **369**, 112625. <https://doi.org/10.1016/j.cam.2019.112625>.
- Mousavi, S.M. and Tahani, M. (2012), "Analytical solution for bending of moderately thick radially functionally graded sector plates with general boundary conditions using multi-term extended Kantorovich method", *Compos. Part B Eng.*, **43**(3), 1405-1416. <https://doi.org/10.1016/j.compositesb.2011.11.068>.
- Nguyen, T.K. (2014), "A higher-order hyperbolic shear deformation plate model for analysis of functionally graded materials", *Int. J. Mech. Mater. Des.*, **11**(2), 203-219. <https://doi.org/10.1007/s10999-014-9260-3>.
- Nikkhoo, A., Asili, S., Sadigh, S., Hajirasouliha, I. and Karegar, H. (2019), "A low computational cost method for vibration analysis of rectangular plates subjected to moving sprung masses", *Adv. Comput. Des.*, **4**(3), 307-326. <https://doi.org/10.12989/acd.2019.4.3.307>.
- Othman, M. and Fekry, M. (2018), "Effect of rotation and gravity on generalized thermo-viscoelastic medium with voids", *Multidisciplin. Model. Mater. Struct.*, **14**(2), 322-338. <https://doi.org/10.1108/MMMS-08-2017-0082>.
- Panda, S.K. and Katariya, P.V. (2015), "Stability and free vibration behaviour of laminated composite panels under thermo-mechanical loading", *Int. J. Appl. Comput. Math.*, **1**, 475-490. <https://doi.org/10.1007/s40819-015-0035-9>.
- Panjehpour, M., Loh, E.W.K. and Deepak, T.J. (2018), "Structural Insulated Panels: State-of-the-Art", *Trends Civ. Eng. Architect.*, **3**(1) 336-340. <https://doi.org/10.32474/TCEIA.2018.03.000151>.
- Pradyumna, S. and Bandyopadhyay, J.N. (2008), "Free vibration analysis of functionally graded curved panels using a higher-order finite element formulation", *J. Sound Vib.*, **318**(1-2), 176-192. <https://doi.org/10.1016/j.jsv.2008.03.056>.
- Reddy, J.N. (2000), "Analysis of functionally graded plates", *Int. J. Numer. Meth. Eng.*, **47**(1-3), 663-684. [https://doi.org/10.1002/\(SICI\)1097-0207\(20000110/30\)47:1/3<663::AID-NME787>3.0.CO;2-8](https://doi.org/10.1002/(SICI)1097-0207(20000110/30)47:1/3<663::AID-NME787>3.0.CO;2-8).
- Rezaiee-Pajand, M. and Karimpour, A. (2020), "Two rectangular elements based on analytical functions", *Adv. Comput. Des.*, **5**(2), 147-175. <https://doi.org/10.12989/acd.2020.5.2.147>.
- Rezaiee-Pajand, M., Masoodi, A.R. and Mokhtari, M. (2018), "Static analysis of functionally graded non-prismatic sandwich beams", *Adv. Comput. Des.*, **3**(2), 165-190. <https://doi.org/10.12989/acd.2018.3.2.165>.
- Safa, A., Hadji, L., Bourada, M. and Zouatnia, N. (2019), "Thermal vibration analysis of FGM beams using an efficient shear deformation beam theory", *Earthq. Struct.*, **17**(3), 329-336. <https://doi.org/10.12989/eas.2019.17.3.329>.
- Safarpour, M., Ghabussi, A., Ebrahimi, F., Habibi, M. and Safarpour, H. (2020), "Frequency characteristics of FG-GPLRC viscoelastic thick annular plate with the aid of GDQM", *Thin-Walled Struct.*, **150**, 106683. <https://doi.org/10.1016/j.tws.2020.106683>.
- Sahouane, A., Hadji, L. and Bourada, M. (2019), "Numerical analysis for free vibration of functionally graded beams using an original HSDT", *Earthq. Struct.*, **17**(1), 31-37. <https://doi.org/10.12989/eas.2019.17.1.031>.
- Sedighi, H.M. and Shirazi, K.H. (2013), "Vibrations of micro-beams actuated by an electric field via parameter expansion method", *Acta Astronautica.*, **85**, 19-24. <https://doi.org/10.1016/j.actaastro.2012.11.014>.
- Sedighi, H.M., Keivani, M. and Abadyan, M. (2015), "Modified continuum model for stability analysis of asymmetric FGM double-sided NEMS: Corrections due to finite conductivity, surface energy and nonlocal effect", *Compos. Part B Eng.*, **83**, 117-133. <https://doi.org/10.1016/j.compositesb.2015.08.029>.
- Selmi, A. (2019), "Effectiveness of SWNT in reducing the crack effect on the dynamic behavior of aluminium alloy", *Adv. Nano Res.*, **7**(5), 365-377. <https://doi.org/10.12989/anr.2019.7.5.365>.
- Shokravi, M. (2017), "Buckling analysis of embedded laminated plates with agglomerated CNT-reinforced composite layers using FSDT and DQM", *Geomech. Eng.*, **12**(2), 327-346. <https://doi.org/10.12989/gae.2017.12.2.327>.
- Shokrieh, M.M. and Kondori, M.S. (2020), "Effects of adding graphene nanoparticles in decreasing of residual stresses of carbon/epoxy laminated composites", *Compos. Mater. Eng.*, **2**(1), 53-64. <https://doi.org/10.12989/cme.2020.2.1.053>.
- Singh, A. and Kumari, P. (2020), "Analytical free vibration solution for angle-ply piezolaminated plate under cylindrical bending: A piezo-elasticity approach", *Adv. Comput. Des.*, **5**(1), 55-89. <https://doi.org/10.12989/acd.2020.5.1.055>.
- Sobhy, M. (2013), "Buckling and free vibration of exponentially graded sandwich plates resting on elastic foundations under various boundary conditions", *Compos. Struct.*, **99**, 76-87. <https://doi.org/10.1016/j.compstruct.2012.11.018>.
- Sobhy, M. (2016), "An accurate shear deformation theory for vibration and buckling of FGM sandwich plates in hygrothermal environment", *Int. J. Mech. Sci.*, **110**, 62-77. <https://doi.org/10.1016/j.ijmecsci.2016.03.003>.
- Sofiyev, A.H., Alizada, A.N., Akin, Ö., Valiyev, A., Avcar, M. and Adiguzel, S. (2012), "On the stability of FGM shells subjected to combined loads with different edge conditions and resting on elastic foundations", *Acta Mech.*, **223**(1), 189-204. <https://doi.org/10.1007/s00707-011-0548-1>.
- Soldatos, K.P. (1992), "A transverse shear deformation theory for homogeneous monoclinic plates", *Acta Mech.*, **94**(3), 195-220. <https://doi.org/10.1007/BF01176650>.
- Swaminathan, K. and Naveenkumar, D.T. (2014), "Higher order refined computational models for the stability analysis of FGM plates – Analytical solutions", *Eur. J. Mech. A Solids*, **47**, 349-361. <https://doi.org/10.1016/j.euromechsol.2014.06.003>.
- Talha, M. and Singh, B.N. (2010), "Static response and free vibration analysis of FGM plates using higher order shear deformation theory", *Appl. Math Modell.*, **34**(12), 3991-4011. <https://doi.org/10.1016/j.apm.2010.03.034>.
- Timesli, A. (2020), "An efficient approach for prediction of the nonlocal critical buckling load of double-walled carbon nanotubes using the nonlocal Donnell shell theory", *SN Appl. Sci.*, **2**, 407. <https://doi.org/10.1007/s42452-020-2182-9>.
- Touratier, M. (1991), "An efficient standard plate theory", *Int. J. Eng. Sci.*, **29**(8), 901-916. [https://doi.org/10.1016/0020-7225\(91\)90165-Y](https://doi.org/10.1016/0020-7225(91)90165-Y).
- Yaghoobi, H. and Yaghoobi, P. (2013), "Buckling analysis of sandwich plates with FGM face sheets resting on elastic foundation with various boundary conditions: An analytical approach", *Meccanica*, **48**, 2019-2035. <https://doi.org/10.1007/s11012-013-9720-0>.
- Yaylaci, M., Terzi, C. and Avcar, M. (2019), "Numerical analysis of the receding contact problem of two bonded layers resting on an elastic half plane", *Struct. Eng. Mech.*, **72**(6), 775-783. <https://doi.org/10.12989/sem.2019.72.6.775>.
- Yüksel, Y.Z. and Akbaş, Ş.D. (2019), "Buckling analysis of a fiber reinforced laminated composite plate with porosity", *J. Comput. Appl. Mech.*, **50**(2), 375-380. <https://doi.org/10.22059/JCAMECH.2019.291967.448>.
- Zhang, B., He, Y., Liu, D., Shen, L. and Lei, J. (2015), "Free vibration analysis of four-unknown shear deformable functionally graded cylindrical microshells based on the strain gradient elasticity theory", *Compos. Struct.*, **119**, 578-597. <https://doi.org/10.1016/j.compstruct.2014.09.032>.
- Zouatnia, N. and Hadji, L. (2019), "Effect of the micromechanical models on the bending of FGM beam using a new hyperbolic

- shear deformation theory”, *Earthq. Struct.*, **16**(2), 177-183.
<https://doi.org/10.12989/eas.2019.16.2.177>.
- Zouatnia, N., Hadji, L. and Kassoul, A. (2018), “An efficient and simple refined theory for free vibration of functionally graded plates under various boundary conditions”, *Geomech. Eng.*, **16**(1), 1-9. <https://doi.org/10.12989/gae.2018.16.1.001>.

CC